Square-Contact Representations of Partial 2-Trees and Triconnected Simply-Nested Graphs*†

Giordano Da Lozzo[1], William E. Devanny[2], David Eppstein[3], and Timothy Johnson[4]

1 Computer Science Department, University of California, Irvine, USA
gdalozzo@uci.edu
2 Computer Science Department, University of California, Irvine, USA
wdevanny@uci.edu
3 Computer Science Department, University of California, Irvine, USA
eppstein@uci.edu
4 Computer Science Department, University of California, Irvine, USA
tujohnso@uci.edu

Abstract

A *square-contact representation* of a planar graph $G = (V, E)$ maps vertices in V to interior-disjoint axis-aligned squares in the plane and edges in E to adjacencies between the sides of the corresponding squares. In this paper, we study *proper* square-contact representations of planar graphs, in which any two squares are either disjoint or share infinitely many points.

We characterize the partial 2-trees and the triconnected cycle-trees allowing for such representations. For partial 2-trees our characterization uses a simple forbidden subgraph whose structure forces a separating triangle in any embedding. For the triconnected cycle-trees, a subclass of the triconnected simply-nested graphs, we use a new structural decomposition for the graphs in this family, which may be of independent interest. Finally, we study square-contact representations of general triconnected simply-nested graphs with respect to their outerplanarity index.

1998 ACM Subject Classification G.2.2 Graph Theory

Keywords and phrases Square-Contact Representations, Partial 2-Trees, Simply-Nested Graphs

Digital Object Identifier 10.4230/LIPIcs.ISAAC.2017.24

1 Introduction

Contact representations of graphs, in which the vertices of a graph are represented by non-overlapping or non-crossing geometric objects of a specific type, and edges are represented by tangencies or other contacts between these objects, form an important line of research in graph drawing and geometric graph theory. For instance, the Koebe–Andreev–Thurston circle packing theorem states that every planar graph is a contact graph of circles [13]. Other types of contact representations that have been studied include contacts of unit circles [2, 9], line segments [10], circular arcs [1], triangles [8], L-shaped polylines [3], and cubes [7].

* Supported in part by the National Science Foundation under Grants CCF-1228639, CCF-1618301, and CCF-1616248. This article also reports on work supported by the U.S. Defense Advanced Research Projects Agency (DARPA) under agreement no. AFRL FA8750-15-2-0092. The views expressed are those of the authors and do not reflect the official policy or position of the Department of Defense or the U.S. Government.

† A full version of the paper is available at [5], https://arxiv.org/abs/1710.00426.

28th International Symposium on Algorithms and Computation (ISAAC 2017).
Editors: Yoshio Okamoto and Takeshi Tokuyama; Article No. 24; pp. 24:1–24:14
Leibniz International Proceedings in Informatics
LIPICS Schloss Dagstuhl – Leibniz-Zentrum für Informatik, Dagstuhl Publishing, Germany

Schramm's monster packing theorem [11] implies that every planar graph can be represented by the tangencies of translated and scaled copies of any smooth convex body in the plane. However, it is more difficult to use this theorem for non-smooth shapes, such as polygons: when k bodies can meet at a point, the monster theorem may pack them in a degenerate way in which separating k-cycles, and their interiors, shrink to a single point.

In this paper we study one of the simplest cases of contact representations that cannot be adequately handled using the monster theorem: contact systems of axis-parallel squares. We distinguish between *proper* and *improper* contacts: a proper contact representation disallows squares that meet only at their corners, while an *improper* or *weak* contact representation allows corner-corner contacts of squares. These weak contacts may represent edges of the graph, but they are also allowed between squares that should be non-adjacent. The weak contact representations by squares were shown by Schramm [12] to include all of the proper induced subgraphs of maximal planar graphs that have no separating 3-cycles or 4-cycles. However, a characterization of the graphs having proper contact representations by squares remains elusive.

There is a simple necessary condition for the existence of a proper contact representation by squares. No three properly-touching squares can surround a nonzero-area region of the plane. Therefore, if every embedding of a planar graph G with four or more vertices has a separating triangle or a triangle as the outer face, then G cannot have a proper contact representation. Our main results show that this necessary condition is also sufficient for two notable families of planar graphs: partial 2-trees (including series-parallel graphs) and triconnected cycle-trees (including the Halin graphs). However, we show that this necessary condition is not sufficient for the existence of weak and proper square-contact representations of 3-outerplanar and 2-outerplanar triconnected simply-nested graphs.

Due to space limits, full versions of omitted or sketched proofs are provided in [5].

2 Preliminaries

For standard graph theory concepts and definitions related to planar graphs, their embeddings, and connectivity we refer the reader, e.g., to [6] and to [5].

The graphs considered in this paper are planar, finite, simple, and connected. We denote the vertex set V and the edge set E of a graph $G = (V, E)$ by $V(G)$ and $E(G)$, respectively. Let H and G be two graphs. We say that G is H-free if G does not contain a subgraph isomorphic to H. The complete k-partite graph $K_{|V_1|,\dots,|V_k|}$ is the graph $(V = \bigcup_{i=1}^{k} V_i, E = \bigcup_{i<j} V_i \times V_j)$.

Series-parallel graphs and partial 2-trees. A *two-terminal series-parallel* graph G with source s and target t can be recursively defined as follows:

(i) Edge st is a two-terminal series-parallel graph. Let $G_1, \dots, G_k$ be two-terminal series-parallel graphs and let s_i and t_i be the source and the target of G_i, respectively, with $1 \le i \le k$.

(ii) The *series composition* of $G_1, \dots, G_k$ obtained by identifying s_i with t_{i+1}, for $i = 1, \dots, k-1$, is a two-terminal series-parallel graph with source s_k and target t_1; and

(iii) the *parallel composition* of $G_1, \dots, G_k$ obtained by identifying s_i with s_1 and t_i with t_1, for $i = 2, \dots, k$, is a two-terminal series-parallel graph with source s_1 and target t_1.

A *series-parallel graph* is either a single edge or a two-terminal series-parallel graph with the addition of an edge, called *reference edge* joining s and t. Clearly, series-parallel graphs are 2-connected. A series-parallel graph G with reference edge e is naturally associated with a rooted tree T, called the *SPQ*-tree of G. Each internal node of T, with the exception of the one associated with e, corresponds to a two-terminal series-parallel graph. Nodes of T are of three types: *S*-, *P*-, and *Q-nodes*. Further, tree T is rooted to the Q-node corresponding to e.

Let μ be a node of T with terminals s and t and children $\mu_1, \dots, \mu_k$, if any. Node μ has an associated multigraph, called the *skeleton* of μ and denoted by $skel_\mu$, containing a *virtual edge* $e_i = s_i t_i$, for each child μ_i of μ. Skeleton $skel_\mu$ shows how the children of μ, represented by "virtual edges", are arranged into μ. The skeleton $skel_\mu$ of μ is:

(i) edge st, if μ is a leaf Q-node,
(ii) the multi-edge obtained by identifying the source s_i and the target t_i of each virtual edge e_i, for $i = 1, \dots, k$, with a new source s and and new target t, respectively, or
(iii) the path $e_1, \dots, e_k$, where virtual edge e_i and e_{i+1} share vertex $s_i = t_{i+1}$, with $1 \le i < k$.

If μ is an S-node, then we denote by $\ell(\mu)$ the length of $skel_\mu$, i.e., $\ell(\mu) = k$.

For each virtual edge e_i of $skel_\mu$, recursively replace e_i with the skeleton $skel_{\mu_i}$ of its corresponding child μ_i. The two-terminal series-parallel subgraph of G that is obtained in this way is the *pertinent graph* of μ and is denoted by G_μ. We have that G_μ is:

(i) edge st, if μ is a Q-node,
(ii) the series composition of the two-terminal series-parallel graphs $G_{\mu_1}, \dots, G_{\mu_k}$, if μ is an S-node, and
(iii) the parallel composition of the two-terminal series-parallel graphs $G_{\mu_1}, \dots, G_{\mu_k}$, if μ is a P-node.

We denote by G^-_μ the subgraph of G_μ obtained by removing from it terminals s and t together with their incident edges.

A 2-*tree* is a graph that can be obtained from an edge by repeatedly adding a new vertex connected to two adjacent vertices. Every 2-tree is planar and 2-connected. A *partial* 2-*tree* is a subgraph of a 2-tree. Equivalently, *partial* 2-*tree* can be defined as the K_4-minor-free graphs. In particular, the series-parallel graphs are exactly the 2-connected partial 2-trees.

Simply-nested graphs. Let G be an embedded planar graph and let $G_1, \dots, G_k$ be the sequence of embedded planar graphs such that $G_1 = G$, graph G_{i+1} is obtained from G_i be removing all the vertices incident to the outer face of G_i together with their incident edges, and G_k is outerplanar. We say that the embedding of G is *k-outerplanar.* A graph is *k-outerplanar* if it admits a k-outerplanar embedding. The set V_i of vertices incident to the outer face of G_i is the *i-th level* of G. A k-outerplanar graph is *simply-nested* [4] if, for $i = 1, \dots, k-1$, graphs $G[V_i]$ are chordless cycles and $G[V_k]$ is either a cycle or a tree.

We define *cycle-trees* and *cycle-cycles* the 2-outerplanar simply-nested graphs whose internal level is a tree and a cycle, respectively. The 2-outerplanar 3-connected simply-nested graphs have a nice geometric interpretation. Similarly to the Halin graphs, which are the graphs of polyhedra containing a face that share an edge with all other faces, 3-connected cycle-trees are the graphs of polyhedra containing a face touched by all other faces. Analogously, the 3-connected cycle-cycle graphs with no chords on the inner cycle are the graphs of polyhedra in which there exist two disjoint faces that are both touched by all other faces.

Square-contact representations. Let $G = (V, E)$ be a planar graph. A *square-contact representation* Γ of G maps each vertex $v \in V$ to an axis-aligned square $S_\Gamma(v)$ in the plane, such that, for any two vertices $u, v \in V$, squares $S_\Gamma(u)$ and $S_\Gamma(v)$ are interior-disjoint, and the sides of $S_\Gamma(u)$ and $S_\Gamma(v)$ touch if and only if $uv \in E$. A square-contact representation of G is *proper* if any two touching squares share infinitely many points, i.e., they cannot share only a corner point, and *non-proper*, otherwise. When the square-contact representation is clear from the context, we may choose to drop the Γ subscript and just use $S(v)$ to refer to the square for vertex v. In the remainder of the paper, we only consider proper square-contact representations and refer to such representations simply as square-contact representations.

Geometric transformations. Let G be planar graph and let Γ be a square-contact representation of G. Also, let p be any point in Γ. We define the $\nearrow$-, $\nwarrow$-, $\swarrow$-, and $\searrow$-*quadrant of* p in Γ as the first, second, third, and fourth quadrant around p, respectively. Suppose that the half-lines delimiting the $\swarrow$-quadrant of p in Γ do not intersect the interior of any square in Γ. Also, let Γ' be the part of Γ lying in the $\swarrow$-quadrant of p. Then, a $\overset{\swarrow}{p}$*-scaling* of Γ *by a factor* $\alpha > 0$ is a square-contact representation Γ^* defined as follows; see, e.g., Fig. 3. Initialize $\Gamma^* = \Gamma$ and remove from Γ^* the drawing of the squares contained in the interior of Γ'. Then, insert into Γ^* a copy Γ'' of Γ' scaled by α such that the upper-right corner of Γ'' coincides with p. Clearly, depending on the scale factor α, drawing Γ^* may or may not be a square-contact representation of G (as adjacencies may be lost or gained). In the following, we refer to the case in which $\alpha > 1$ simply as a $\overset{\swarrow}{p}$*-scaling* of Γ and to the case in which $0 < \alpha < 1$ as a *negative* $\overset{\swarrow}{p}$*-scaling* of Γ. The definitions of $\overset{\circ}{p}$*-scaling* and *negative* $\overset{\circ}{p}$*-scaling*, with $\circ \in \{\nwarrow, \searrow, \nearrow\}$, are analogous. Finally, let v be a vertex of G and let x, y, z, and w be the upper-left, lower-left, lower-right, and upper-left corner points of $S(v)$ in Γ. A $\overset{\nwarrow}{v}$*-scaling*, $\overset{\swarrow}{v}$*-scaling*, $\overset{\searrow}{v}$*-scaling*, $\overset{\nearrow}{v}$*-scaling* of Γ is a $\overset{\nwarrow}{x}$*-scaling*, $\overset{\swarrow}{y}$*-scaling*, $\overset{\searrow}{z}$*-scaling*, $\overset{\nearrow}{w}$*-scaling* of Γ, respectively.

3 Partial 2-Trees

In this section, we study square-contact representations of partial 2-trees and give the following simple characterization for graphs in this family admitting such representations.

▶ **Theorem 1.** *Let G be a partial 2-tree. Then, the following statements are equivalent:*
(i) *G is $K_{1,1,3}$-free,*
(ii) *G admits an embedding without separating triangles, and*
(iii) *G admits a square-contact representation.*

In order to prove Theorem 1, we first show that, without loss of generality, we can restrict our attention to the biconnected partial 2-trees, i.e., the series-parallel graphs.

▶ **Lemma 1.** *Let G be a $K_{1,1,3}$-free partial 2-tree. Then, there exists a $K_{1,1,3}$-free series-parallel graph G^* such that $G \subset G^*$ and G admits a square-contact representation if G^* does.*

Sketch. Let $\beta(H)$ denote the number of blocks, i.e., the maximal biconnected components, of a graph H. Adding to G a new vertex connected to two vertices in $V(G)$ incident to the same cut-vertex of G, belonging to different blocks, and sharing a common face yields a graph G' such that $\beta(G') = \beta(G) - 1$. It is easy to see that G' is $K_{1,1,3}$-free and that G' does not contain K_4 as a minor. Hence, repeating such an augmentation eventually yields a series-parallel graph G^* that is $K_{1,1,3}$-free. Also, by construction, two vertices in $V(G)$ are adjacent in G^* if and only if they are adjacent in G. Therefore, a square-contact representation of G can be derived from a square-contact representation Γ^* of G^*, by removing from Γ^* all the squares corresponding to vertices in $V(G^*) \setminus V(G)$. ◀

As already observed in Section 1, an embedding without separating triangles is necessary for the existence of a square-contact representation, and $K_{1,1,3}$ has no embedding without separating triangles. Thus, $(iii) \Rightarrow (ii) \Rightarrow (i)$ are immediate. To complete the proof of Theorem 1, we show how to construct a square-contact representation of any $K_{1,1,3}$-free series-parallel graph, proving that $(i) \Rightarrow (iii)$. We formalize this result in the next theorem.

▶ **Theorem 2.** *Every $K_{1,1,3}$-free series-parallel graph admits a square-contact representation.*

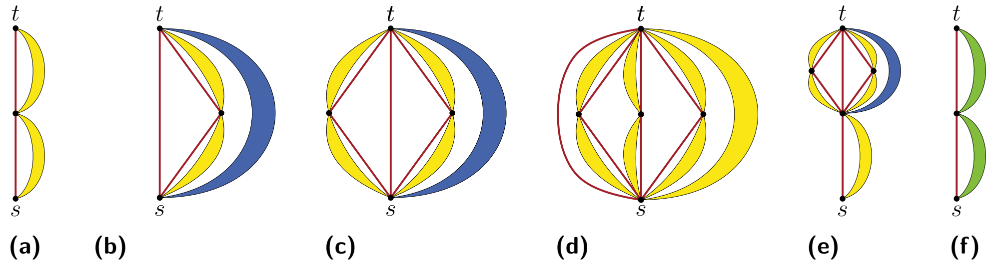

Figure 1 (a) A critical S-node, (b) an almost-bad P-node, (c) a bad P-node, (d) a forbidden P-node, (e) an S-node of `Type B`, and (f) an S-node of `Type C`. Yellow, green, and blue regions represent parallel compositions of any number of S-nodes, at most one critical S-node and any number of non-critical S-nodes, and any number of non-critical S-nodes, respectively.

Let G be a series-parallel graph and let T be the SPQ-tree of G with respect to any reference edge. We start with some definitions; refer to Fig. 1. Let μ be an S-node in T. We say that μ is *critical*, if $skel_\mu = s$–x–t and the two children of μ both contain an edge between their terminals, i.e., $sx, xt \in E(G_\mu)$, and *non-critical*, otherwise. Let μ be a P-node in T containing an edge between its terminals. We say that μ is *almost bad*, if it has exactly one critical child, *bad*, if it has exactly two critical children, and *forbidden*, if it has more than two critical children. Finally, let μ be a P-node in T. We say that μ is *good*, if it is neither bad, nor almost bad, nor forbidden.

We now assign one of three possible types to each S-node μ in T as follows (for each child μ_i of μ, we denote the two terminals of G_{μ_i} as s_i and t_i).

Type A Node μ is of `Type A`, if either $\ell(\mu) > 2$ or $\ell(\mu) = 2$ and at least one child of μ does not contain an edge between its terminals, i.e., $|\{s_1t_1, s_2t_2\} \cap E(G_\mu)| < 2$.

Type B Node μ is of `Type B`, if $\ell(\mu) = 2$, all its children contain an edge between their terminals, and at least one of them is a bad P-node.

Type C Node μ is of `Type C`, if $\ell(\mu) = 2$, and all its children contain an edge between their terminals, and none of them is a bad P-node.

Observe that S-nodes of `Type B` and of `Type C` are also critical.

Let G be a $K_{1,1,3}$-free series-parallel graph and let T be the SPQ-tree of G with respect to any reference edge. We have the following simple observations regarding the P-nodes in T.

▶ **Observation 1.** *SPQ-tree T contains no forbidden P-node; refer to Fig. 1(d).*

▶ **Observation 2.** *Let μ be a P-node in T with terminals s and t such that $st \in E(G_\mu)$. Then, none of the children of μ is of `Type B` and at most two children of μ are of `Type C`.*

We now consider special square-contact representations for the pertinent graphs of the S-nodes in T. Let Γ_μ be a square-contact representation of G_μ. We say that Γ_μ is either a *rectangular*, *L-shape*, or *pipe drawing* of G_μ, if it satisfies the following conditions; refer to Fig. 2.

Rectangular drawing $S(t)$ lies to the left and above $S(s)$ and the drawing Γ^-_μ of G^-_μ in Γ_μ lies to the right of $S(t)$ and above $S(s)$; also, all the squares of Γ^-_μ whose left side (bottom side) is collinear with the right side of $S(t)$ (with the top side of $S(s)$) are adjacent to $S(t)$ (to $S(s)$).

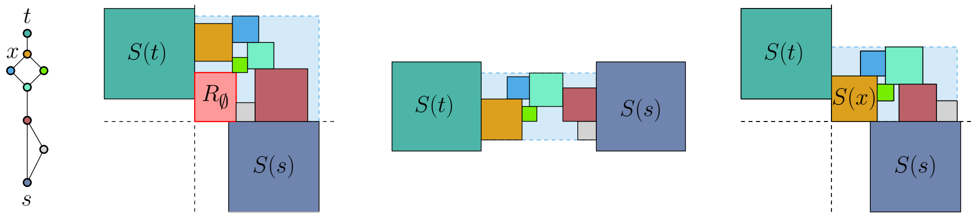

Figure 2 From left to right: pertinent G_μ of an S-node μ with terminals s and t, L-shape and pipe drawings of G_μ, respectively, and a rectangular drawing of an S-node ν with pertinent $G_\nu = G_\mu \cup sx$. The L-shape region and horizontal pipe enclosing G^-_μ and the rectangle enclosing G^-_ν are shaded blue.

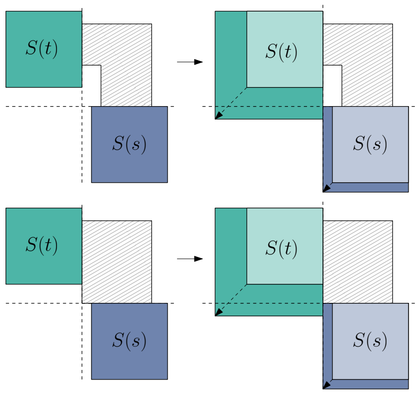

Figure 3 Transforming Γ_τ into Γ_ρ.

L-shape drawing Γ_μ is a rectangular drawing in which there exists a rectangular region (red region $R_\emptyset$ in Fig. 2) inside the bounding box of Γ^-_μ whose interior does not intersect any square in Γ^-_μ and whose lower-left corner lies at the intersection point between the vertical line passing through the right side of $S(t)$ and the horizontal line passing through the top side of $S(s)$.

Pipe drawing $S(t)$ lies to the left of $S(s)$ and the drawing Γ^-_μ of G^-_μ in Γ_μ lies to the right of $S(t)$ and to the left of $S(s)$; also, all the squares of Γ^-_μ whose left side (right side) is collinear with the right side of $S(t)$ (with the left side of $S(s)$) are adjacent to $S(t)$ (to $S(s)$).

In the following, we generally refer to a drawing of an S-node μ in T (of G_μ) which is either an L-shape drawing, a pipe drawing, or a rectangular drawing as a *valid drawing* of μ (of G_μ).

Let Γ^-_μ be the square-contact representation of G^-_μ contained in Γ_μ. Observe that Γ^-_μ lies in the interior of an orthogonal hexagon with an internal angle equal to 270°, i.e., an *L-shape polygon* (or, simply, *L-shape*), if Γ^-_μ is an L-shape drawing. Also, Γ^-_μ lies in the interior of a rectangle whose opposite vertical sides are adjacent to the right side of $S(t)$ and to the left side of $S(s)$, i.e., a *horizontal pipe*, if Γ^-_μ is a pipe drawing. Finally, Γ^-_μ lies in the interior of a rectangle whose left and bottom side are adjacent to the right side of $S(t)$ and to the top side of $S(s)$, respectively, if Γ^-_μ is a rectangular drawing.

Proof of Theorem 2. In order to prove Theorem 2, we proceed as follows. Let G be a $K_{1,1,3}$-free series-parallel graph and let T be the SPQ-tree of G rooted at a Q-node ρ with terminals s and t, whose unique child τ is an S-node. Observe that such a Q-node always exists, since G is simple, and that node τ is either of `Type A` or of `Type C`, since G is $K_{1,1,3}$-tree. We perform a bottom-up traversal in T to construct one or two valid drawings of G_μ, for each S-node $\mu \in T$. Namely, we compute:

- an L-shape drawing, if μ is of `Type A` (Lemma 4),
- a pipe drawing, if μ is of `Type B` (Lemma 5), and
- both a pipe drawing and a rectangular drawing, if μ is of `Type C` (Lemma 6).

Thus, when node τ is considered, we can compute either an L-shape drawing of G_τ, if τ is of `Type A`, or a rectangular drawing of G_τ, if τ is of `Type C`. Further, both such valid drawings Γ_τ of G_τ can be easily turned into a square-contact representation Γ_ρ of $G = G_\tau \cup st$, by performing a $\overset{\swarrow}{t}$-scaling and an $\overset{\swarrow}{s}$-scaling of Γ_τ in such a way that the right side of $S(t)$ and the left side of $S(s)$ touch; refer to Fig. 3. This is possible since both in an L-shape drawing and in a rectangular drawing of G_τ all the squares of G^-_τ whose left side (bottom side) is collinear with the right side of $S(t)$ (with the top side of $S(s)$) are adjacent to $S(t)$ (to $S(s)$).

Let μ be an S-node and let $\mu_1, \dots, \mu_k$ be the children of μ in T. If each child μ_i of μ is a Q-node, then node μ is of `Type A`, if $\ell(\mu) > 2$, and it is of `Type C`, otherwise. It is not difficult to see that, in the former case, G_μ admits an L-shape drawing and that, in the latter case, G_μ admits both a pipe drawing and a rectangular drawing. In the remainder of the section, we consider the case in which μ has both Q-node and P-node children.

We first show how to construct special square-contact representations of G_μ, that we call *canonical drawings*, for any P-node μ in T, assuming that valid drawings have been computed for each S-node child of μ. We distinguish five possible canonical drawings, depending on

1. the number and type of the S-node children of μ and
2. the presence of edge st.

Each canonical drawing has three variants: `vertical` (V), `horizontal` (H), and `diagonal` (D). We name such canonical representations *XY drawings*, where $X \in \{V, H, D\}$ denotes the variant of the representation and $Y = 1$, if $st \in E(G_\mu)$, and $Y = 0$, otherwise. Canonical drawings share the following main property (which, in fact, also holds for valid drawings).

▶ **Property 1.** *Let Γ_μ be a valid drawing or a canonical drawing of G_μ. Then, for each vertex v in $V(G^-_\mu)$, it holds that $vs \in E(G_\mu)$ ($vt \in E(G_\mu)$) if:*
1. *$S(v)$ has a side that is collinear with a side of $S(s)$ (of $S(t)$) in Γ_μ and*
2. *$S(v)$ is separated from $S(s)$ (from $S(t)$) in Γ_μ by the line passing through such a side.*

Property 1 allows us to modify canonical and valid drawings by appropriate $\overset{\circ}{s}$-scaling and $\overset{\circ}{t}$-scaling transformations, with $\circ \in \{\nwarrow, \nearrow, \searrow, \swarrow\}$, preserving adjacencies between vertices in G_μ.

First, consider a P-node μ in T with terminals s and t such that $st \notin E(G_\mu)$ and let $\mu_1, \dots, \mu_k$ be the S-node children of μ. We say that a square-contact representation Γ_μ of G_μ is an *H0 drawing* or a *V0 drawing*, if it satisfies the following conditions (in addition to Property 1); refer to Fig. 4.

H0 drawing $S(t)$ lies to the left of $S(s)$, the bottom side of $S(s)$ lies below the bottom side of $S(t)$, and the drawing of G^-_μ in Γ_μ lies to the right of $S(t)$, below the top side of $S(t)$, above the bottom side of $S(s)$, and to the left of the right side of $S(s)$.

V0 drawing $S(t)$ lies above $S(s)$, the left side of $S(s)$ lies to the right of the left side of $S(t)$, and the drawing of G^-_μ in Γ_μ lies above $S(s)$, to the right of the left side of $S(s)$, below the top side of $S(t)$, and to the left of the right side of $S(s)$.

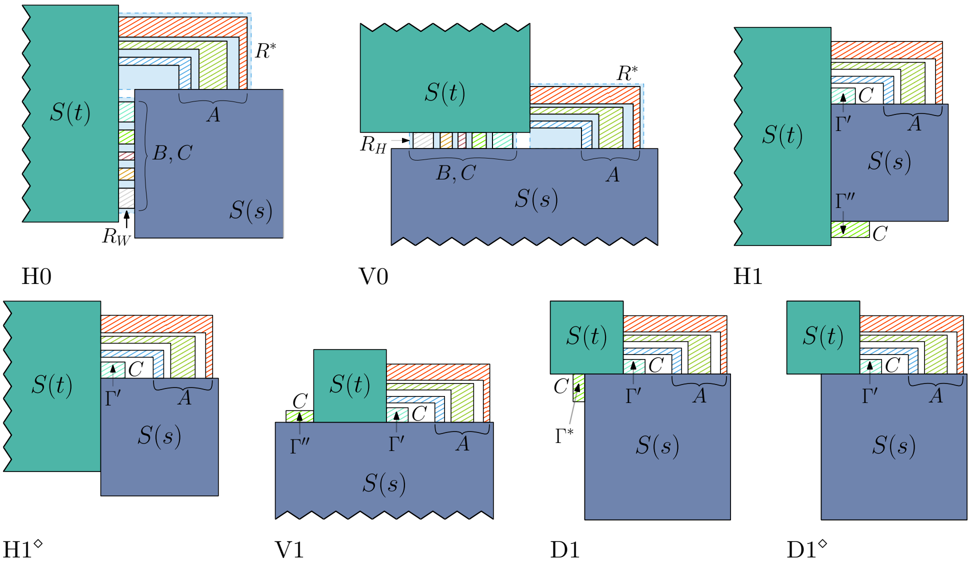

Figure 4 Canonical drawings of a P-node μ. The striped regions correspond to L-shapes, horizontal pipes, and rectangles enclosing the square-contact representations of graphs $G^-_{\mu_i}$, for each S-node child μ_i of μ. Labels A, B, and C indicate the type of each S-node.

Now, consider a P-node μ in T with terminals s and t such that $st \in E(G_\mu)$ and let $\mu_1, \ldots, \mu_k$ be the S-node children of μ. We say that a square-contact representation Γ_μ of G_μ is an *H1 drawing*, an *H1*$^\diamond$ *drawing*, a *V1 drawing*, a *D1 drawing*, or a *D1*$^\diamond$ *drawing*, if it satisfies the following conditions (in addition to Property 1); refer to Fig. 4.

H1 drawing $S(t)$ lies to the left of $S(s)$, the bottom side of $S(s)$ lies above the bottom side of $S(t)$, and the drawing of G^-_μ in Γ_μ lies to the right of $S(t)$, below the top side of $S(t)$, above the bottom side of $S(t)$, and to the left of the right side of $S(s)$.

H1$^\diamond$ **drawing** $S(t)$ lies to the left of $S(s)$, the bottom side of $S(s)$ lies below the bottom side of $S(t)$, and the drawing of G^-_μ in Γ_μ lies to the right of $S(t)$, below the top side of $S(t)$, above the top side of $S(s)$, and to the left of the right side of $S(s)$.

V1 drawing $S(t)$ lies above $S(s)$ and the drawing of G^-_μ in Γ_μ lies above $S(s)$, below the top side of $S(t)$, to the right of the left side of $S(s)$, and to the left of the right side of $S(s)$.

D1 drawing $S(t)$ lies above $S(s)$ and the left side of $S(t)$ lies to the left of the left side of $S(s)$, and the drawing of G^-_μ in Γ_μ lies to the right of the left side of $S(t)$, below the top side of $S(t)$, above the bottom side of $S(s)$, and to the left of the right side of $S(s)$.

D1$^\diamond$ **drawing** Γ_μ is a D1 drawing of G_μ in which the drawing of G^-_μ lies to the right of $S(t)$.

We now present two lemmata for the possible canonical drawings of each P-node μ in T. Recall that, by Observation 1, we can assume that μ is not a forbidden P-node. Let $\mu_1, \ldots, \mu_k$ be the S-node children of μ. The general strategy in the proofs of both lemmata consists of

1. computing appropriate valid drawings $\Gamma_{\mu_1}, \ldots, \Gamma_{\mu_k}$ for the pertinent graphs $G_{\mu_1}, \ldots, G_{\mu_k}$ of $\mu_1, \ldots, \mu_k$, respectively,
2. modifying the square-contact representation of $G^-_{\mu_i}$ contained in Γ_{μ_i}, for $i = 1, \ldots, k$, by means of affine transformations, so that representations derived from S-nodes of the same type lie in the interior of the same polygon, and finally
3. composing the resulting drawings into a canonical drawing of G_μ. Refer to [5] for details.

We first consider the case in which μ does not contain an edge between its terminals. In this case, by Lemmata 4, 5, and 6, we can assume that Γ_{μ_i} is an L-shape drawing, if μ_i is of `Type A`, and a pipe drawing, if μ_i is of `Type B` or of `Type C`, for $i = 1, \dots, k$.

▶ **Lemma 2.** *Let μ be a P-node in T with terminals s and t such that $st \notin E(G_\mu)$. Then, graph G_μ admits an H0 drawing and a V0 drawing.*

Then, we consider the case in which μ contains an edge between its terminals. Recall that, by Observation 2, node μ has no child of `Type B` and at most two children of `Type C`. In particular, node μ has two children of `Type C`, if it is bad, and one child of `Type C`, if it is almost bad. In this case, by Lemmata 4 and 6, we can assume that Γ_{μ_i} is an L-shape drawing, if μ_i is of `Type A`, and a rectangular drawing, if μ_i is of `Type C`, for $i = 1, \dots, k$.

▶ **Lemma 3.** *Let μ be a P-node in T with terminals s and t such that $st \in E(G_\mu)$. Then, graph G_μ admits*

- *an H1 drawing, a V1 drawing, and a D1 drawing, if μ is bad, or*
- *an H1$^\diamond$ drawing and a D1$^\diamond$ drawing, if μ is good or almost bad.*

We finally turn our attention to the valid drawings of the S-nodes in T. Let μ be an S-node in T and let $\mu_1, \dots, \mu_k$ be the children of μ (where the virtual edge e_i, corresponding to node μ_i, precedes the virtual edge e_{i+1}, corresponding to node μ_{i+1}, from t to s in $skel_\mu$). The next three lemmata immediately imply Theorem 2. To simplify their proofs, we assume that each child of μ is a P-node. In fact, the case in which a child of μ is a Q-node can be treated analogously to that of a P-node containing an edge between its terminals. The general strategy in the proofs of all three lemmata consists of

1. computing appropriate canonical drawings $\Gamma_{\mu_1}, \dots, \Gamma_{\mu_k}$ for the pertinent graphs $G_{\mu_1}, \dots, G_{\mu_k}$ of $\mu_1, \dots, \mu_k$, respectively,
2. modifying these drawings, by means of affine transformations, so that the squares corresponding to terminals shared by different children of μ can be identified without introducing any overlapping between squares corresponding to internal vertices of G_{μ_i} and G_{μ_j}, with $i \neq j$, and finally
3. composing the resulting drawings into a valid drawing of G_μ.

▶ **Lemma 4.** *If μ is an S-node of `Type A`, then G_μ admits an L-shape drawing.*

Proof. We first describe how to select a valid drawing of Γ_{μ_i} of G_{μ_i}, for $i = 1, \dots, k$, based on whether (i) $\ell(\mu) > 2$ or (ii) $\ell(\mu) = 2$. Recall that, if $\ell(\mu) = 2$, then at least one child of μ does not contain an edge between its terminals, say μ_1 (the case in which $s_1t_1 \in E(G_{\mu_1})$ and $s_2t_2 \notin E(G_{\mu_2})$ is analogous).

(i) By Lemma 2 and Lemma 3, we can construct a drawing Γ_{μ_i}, for each μ_i, such that:
  1. Γ_{μ_1} is an H0 drawing, if $s_1t_1 \notin E(G_{\mu_1})$, and Γ_{μ_1} is an H1 drawing (H1$^\diamond$ drawing), if μ_1 is bad (if μ_1 is good or almost bad);
  2. Γ_{μ_2} is a V0 drawing, if $s_2t_2 \notin E(G_{\mu_2})$, and Γ_{μ_2} is a D1 drawing (D1$^\diamond$ drawing), if μ_2 is bad (if μ_2 is good or almost bad); and
  3. Γ_{μ_i} is a V0 drawing, if $s_it_i \notin E(G_{\mu_i})$, and Γ_{μ_i} is a V1 drawing (D1$^\diamond$ drawing), if μ_i is bad (if μ_i is good or almost bad), for every $i > 2$.

(ii) By Lemma 2 and Lemma 3, we can construct an H0 drawing Γ_{μ_1} of G_{μ_1} and a V1 drawing (D1$^\diamond$ drawing) Γ_{μ_2} of G_{μ_2}, if μ_2 is bad (if μ_2 is good or almost bad).

We show how to compose all such drawings into an L-shape drawing Γ_μ of G_μ as follows. Refer to Fig. 5(a) for an example of how to compose drawings Γ_{μ_i}, with $i = 1, \dots, k$, in case (i) and to Fig. 5(b) for an example of how to compose drawings Γ_{μ_1} and Γ_{μ_2} in case (ii). First,

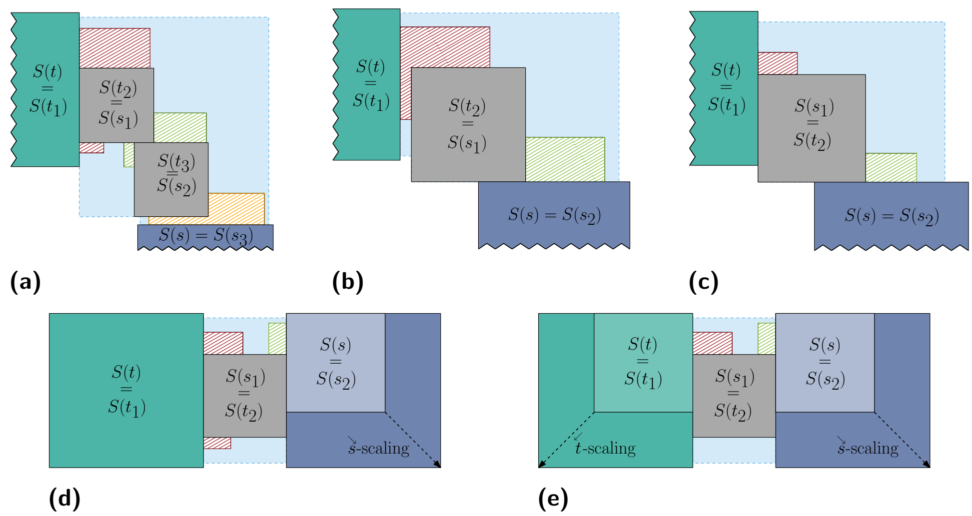

Figure 5 Illustrations for the proofs of Lemmata 4, 5, and 6. Striped polygons of the same color enclose different parts of the drawing of each graph $G^-_{\mu_i}$ (contained in the canonical drawing Γ_{μ_i} of G_{μ_i}). (a) An H1 drawing of G_{μ_1}, a D1 drawing of G_{μ_2}, and a D1$^\diamond$ drawing of G_{μ_3} are combined into an L-shape drawing. (b) An H0 drawing of G_{μ_1} and a D1$^\diamond$ drawing of G_{μ_2} are combined into an L-shape drawing. (c) An H1$^\diamond$ drawing of G_{μ_1} and a D1$^\diamond$ drawing of G_{μ_2} are combined into a rectangular drawing. (d) An H1 drawing of G_{μ_1} and a D1$^\diamond$ drawing of G_{μ_2} are combined into a pipe drawing. (e) An H1$^\diamond$ drawing of G_{μ_1} and a D1$^\diamond$ drawing of G_{μ_2} are combined into a pipe drawing.

we scale $S(s_i)$ and $S(t_i)$ in Γ_{μ_i} so that the bounding box of the drawing of each connected component of $G_{\mu_i} - \{s_i, t_i\}$ in Γ_{μ_i}, for $i = 1, \dots, k$, becomes arbitrarily small with respect to the drawing of $S(s_i)$ and $S(t_i)$. This avoids overlapping between internal vertices of G_{μ_i} and G_{μ_j}, with $i \neq j$, in the next phases of the construction. Then, we scale and translate each drawing Γ_{μ_i} so that $S(t_{i+1}) = S(s_i)$, with $i < k$. It is easy to see that, by the choice of the canonical drawings of each G_{μ_i}, there exists a rectangular region in Γ_μ whose interior does not intersect any square representing a vertex in G^-_μ and whose lower-left corner lies at the intersection point between the vertical line passing through the right side of $S(t)$ and the horizontal line passing through the top side of $S(s)$ in Γ_μ. ◀

The proof of the next two lemmata also exploits rotations of drawings Γ_{μ_i} and can be carried out in a fashion similar to the proof of Lemma 4. Refer to [5] for details.

▶ **Lemma 5.** *If μ is an S-node of* `Type B`*, then G_μ admits a pipe drawing.*

▶ **Lemma 6.** *If μ is an S-node of* `Type C`*, then G_μ admits a pipe and a rectangular drawing.*

4 Triconnected Simply-Nested Graphs

In this section, we devote our attention to 3-connected simply-nested graphs.

A cycle-tree with a single edge removed from the outer cycle is a *path-tree* (to avoid special cases, we allow the outer cycle of the cycle-tree to be a 2-gon). In path-trees, we refer to vertices in the tree as *tree vertices* and vertices in the external path as *path vertices*. A tree vertex can *see* a path vertex if they share a face in the original cycle-tree. Define an *almost-triconnected path-tree with root ρ, leftmost path vertex ℓ, and rightmost path vertex r* to be a path-tree containing in one of its faces a tree vertex ρ and path vertices ℓ and r such that if the edges $\rho\ell$, ρr, and ℓr were added, the resulting graph would be a 3-connected cycle-tree.

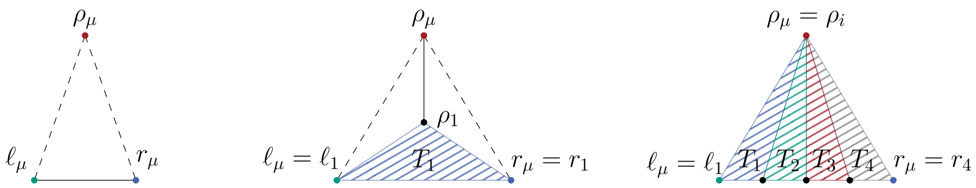

Figure 6 Path-trees associated with a Q-node (left), an S-node (middle), and a P-node (right). Dashed edges may or may not exist. Striped triangles represent smaller path-trees T_i with root ρ_i.

SPQ-decomposition of path-trees. We now describe a recursive decomposition for almost-triconnected path-trees. We call this an SPQ-decomposition, because it bears a striking similarity to the SPQ-decomposition of series-parallel graphs. Let G be a 3-connected cycle-tree, let ℓr be an edge incident to the outer cycle of G, and let ρ be a tree vertex incident to the internal face of G edge ℓr is incident to. Also, let $G' = G - \ell r$ be the almost-triconnected path-tree obtained from G by removing edge ℓr. Graph G' defines a rooted decomposition tree T whose nodes are of three different kinds: *S-*, *P-*, and *Q-nodes*. Each node μ of T is associated with a path-tree G_μ with root ρ_μ, leftmost path vertex ℓ_μ, and rightmost path vertex r_μ obtained—except the Q-nodes—from smaller path-trees T_i with root ρ_i, leftmost path vertex ℓ_i, and rightmost path vertex r_i, for $i = 1, \dots, k$, as follows.

- A *Q-node* μ is associated with a path-tree G_μ with three vertices: one tree vertex ρ_μ and two path vertices ℓ_μ and r_μ. The tree vertex ρ_μ is the root of G_μ, while path vertices ℓ_μ and r_μ are the leftmost and the rightmost path vertex of G_μ, respectively. Edge $\ell_\mu r_\mu$ will always exist, but edges $\rho_\mu \ell_\mu$ and $\rho_\mu r_\mu$ may or may not exist; see Fig. 6(left).
- An *S-node* μ is associated with a path-tree G_μ obtained from path-tree T_1 by adding a new root ρ_μ connected to ρ_1. Also, $\ell_\mu = \ell_1$ and $r_\mu = r_1$ are the leftmost and the rightmost path vertex of G_μ, respectively. Edges $\rho_\mu \ell_\mu$ and $\rho_\mu r_\mu$ may or may not exist; see Fig. 6(midde).
- A *P-node* μ is associated with a path-tree G_μ obtained from path-trees T_i by merging $T_1, T_2, \dots, T_k$ from left to right as follows. First, roots ρ_i are identified into a new root ρ_μ. Then, the rightmost path vertex r_i of T_i and the leftmost path vertex ℓ_{i+1} of T_{i+1} are identified, for $i = 1, \dots, k-1$. Path vertices $\ell_\mu = \ell_1$ and $r_\mu = r_k$ are the leftmost and the rightmost path vertex of G_μ, respectively; see Fig. 6(right).

We have the following lemma.

▶ **Lemma 7.** *Any almost-triconnected path-tree admits an SPQ-decomposition.*

In [5] we show how to construct a square-contact representation of any almost-triconnected path-tree G without separating triangles and whose outer face is not a triangle by inductively maintaining the invariant depicted in Fig. 7 for the S- and P-nodes of an SPQ-decomposition of G. We formalize this result in the next lemma.

▶ **Lemma 8.** *Any almost-triconnected path-tree G without separating triangles and whose outer face is not a triangle admits a square-contact representation.*

To construct a square-contact representation for a 3-connected cycle-tree, it is natural to remove an edge in the outer cycle to obtain a path-tree, use Lemma 8 to construct a square-contact representation, and then attempt to reintroduce a contact for the removed edge. However, because Lemma 8 places the leftmost and rightmost path vertices on the left and right side of the drawing, it is unclear how to add a contact between them. Instead,

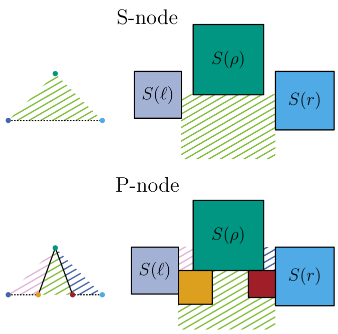

Figure 7 Invariants for S- and P-nodes with more than two path vertices.

we split the cycle-tree into two overlapping almost-triconnected path-trees, obtain their square-contact representations by Lemma 7, and overlay them to form a square-contact representation for the entire cycle-tree.

▶ **Theorem 3.** *Any* 3*-connected cycle-tree* G *without separating triangles and whose outer face is not a triangle admits a square-contact representation.*

As Halin graphs are 3-connected cycle-trees without separating triangles and have, except for K_4, a non-triangular outer face, we have the following.

▶ **Corollary 4.** *Any Halin graph* $G \not\simeq K_4$ *admits a square-contact representation.*

Next, we investigate square-contact representations of 2-outerplanar simply-nested graphs that are not cycle-trees (Theorem 5) and 3-outerplanar simply nested graphs (Theorem 6).

▶ **Theorem 5.** *There exists a* 3*-connected* 2*-outerplanar simply-nested graph that does not admit any proper square-contact representation.*

Proof. Consider the two nested quadrilaterals shown in Fig. 8(left). One of its two quadrilateral faces must be the outer one, giving the embedding shown. In any square-contact representation, the inner polygon surrounded by the squares for the four outer vertices must be a rectangle, as it has only four sides. Each of the four inner squares must touch one of the four corners of this rectangle (the corner made by its two outer neighbors). For the four inner squares to touch the four corners of the rectangle and each other, the only possibility is that the rectangle is a square and each inner square fills one quarter of it, as shown in Fig. 8(middle). However, this representation is improper, as diagonally-opposite inner squares meet at their corners. ◀

▶ **Theorem 6.** *There exists a* 3*-connected* 3*-outerplanar simply-nested graph that does not admit any square-contact representation.*

Proof. Consider the graph shown in Fig. 8(right). Its quadrilateral face must be the outer one, giving the embedding shown. As in the proof of Theorem 5, the only possible representation for its two outer quadrilaterals has the four outer squares surrounding a central square region, divided into four quarters representing the four middle vertices, as shown in Fig. 8(middle). However, this representation leaves no room for the inner vertex. ◀

We remark that the graph of Theorem 6 is actually 2-outerplanar simply-nested, but not with its quadrilateral face as the outer face.

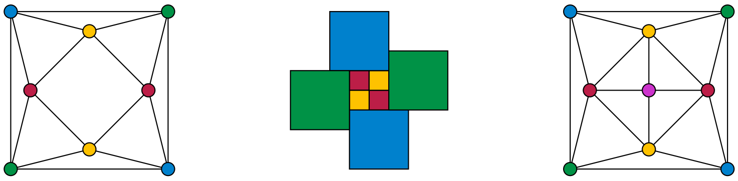

Figure 8 Left: Two nested quadrilaterals form a graph with no proper square-contact representation. Middle: An improper square-contact representation for the same graph. Right: A graph with no square-contact representation, even an improper one.

5 Conclusions

In this paper, we provided simple characterizations for two notable families of planar graphs that admit proper square-contact representations. Moreover, we introduced a new decomposition for an interesting family of polyhedral graphs that generalize the Halin graphs, i.e., the 3-connected cycle-trees. Finally, we showed that the absence of separating triangles and a non-triangular outer face do not guarantee the existence of weak and proper square-contact representations of 3-outerplanar and 2-outerplanar simply-nested graphs, respectively.

Acknowledgements. We thank Jawaherul M. Alam for useful discussions on this subject.

References

1 Md. Jawaherul Alam, David Eppstein, Michael Kaufmann, Stephen G. Kobourov, Sergey Pupyrev, André Schulz, and Torsten Ueckerdt. Contact graphs of circular arcs. In *WADS '15*, volume 9214 of *LNCS*, pages 1–13. Springer, 2015. doi:10.1007/978-3-319-21840-3_1.

2 Clinton Bowen, Stephane Durocher, Maarten Löffler, Anika Rounds, André Schulz, and Csaba D. Tóth. Realization of simply connected polygonal linkages and recognition of unit disk contact trees. In *GD '15*, volume 9411 of *LNCS*, pages 447–459. Springer, 2015. doi:10.1007/978-3-319-27261-0_37.

3 Steven Chaplick, Stephen G. Kobourov, and Torsten Ueckerdt. Equilateral l-contact graphs. In *WG '13*, volume 8165 of *LNCS*, pages 139–151. Springer, 2013. doi:10.1007/978-3-642-45043-3_13.

4 Robert J. Cimikowski. Finding hamiltonian cycles in certain planar graphs. *Inf. Process. Lett.*, 35(5):249–254, 1990. doi:10.1016/0020-0190(90)90053-Z.

5 Giordano Da Lozzo, William Devanny, David Eppstein, and Timothy Johnson. Square-contact representations of partial 2-trees and triconnected simply-nested graphs. Tech. Report arXiv:1710.00426, Cornell University, 2017. URL: http://arxiv.org/abs/1710.00426.

6 Giuseppe Di Battista, Peter Eades, Roberto Tamassia, and Ioannis G. Tollis. *Graph Drawing: Algorithms for the Visualization of Graphs.* Prentice-Hall, 1999.

7 Stefan Felsner and Mathew C. Francis. Contact representations of planar graphs with cubes. In *SoCG '11*, pages 315–320. ACM, 2011. doi:10.1145/1998196.1998250.

8 Daniel Gonçalves, Benjamin Lévêque, and Alexandre Pinlou. Triangle contact representations and duality. *Discrete Comput. Geom.*, 48(1):239–254, 2012. doi:10.1007/s00454-012-9400-1.

9 H. Harborth. Lösung zu Problem 664A. *Elemente der Mathematik*, 29:14–15, 1974.

10 Petr Hliněný. Contact graphs of line segments are NP-complete. *Discrete Math.*, 235(1-3):95–106, 2001. doi:10.1016/S0012-365X(00)00263-6.

11 Oded Schramm. *Combinatorically Prescribed Packings and Applications to Conformal and Quasiconformal Maps.* PhD thesis, Princeton University, 1990.

12 Oded Schramm. Square tilings with prescribed combinatorics. *Israel J. Math.*, 84(1-2):97–118, 1993. doi:10.1007/BF02761693.

13 Kenneth Stephenson. *Introduction to Circle Packing: The theory of discrete analytic functions.* Cambridge University Press (1), 2005.